



Article

# Effects of Cobra Cardiotoxins on Intracellular Calcium and the Contracture of Rat Cardiomyocytes Depend on Their Structural Types

Alexey S. Averin <sup>1</sup>, Alexey V. Berezhnov <sup>1</sup> , Oleg Y. Pimenov <sup>2</sup>, Miliausha H. Galimova <sup>2</sup>, Vladislav G. Starkov <sup>3</sup>, Victor I. Tsetlin <sup>3</sup> and Yuri N. Utkin <sup>3,\*</sup>

<sup>1</sup> Institute of Cell Biophysics, Federal Research Center “Pushchino Scientific Center of Biological Research”, Pushchino Branch, Russian Academy of Sciences, Pushchino 142290, Russia; averinas82@gmail.com (A.S.A.); alexber56@gmail.com (A.V.B.)

<sup>2</sup> Institute of Theoretical and Experimental Biophysics, Russian Academy of Sciences, Pushchino 142290, Russia; plegiteb@gmail.com (O.Y.P.); mgalimova@mail.ru (M.H.G.)

<sup>3</sup> Shemyakin–Ovchinnikov Institute of Bioorganic Chemistry, Russian Academy of Sciences, Moscow 117997, Russia; vladislavstarkov@mail.ru (V.G.S.); victortsetlin3f@gmail.com (V.I.T.)

\* Correspondence: utkin@mx.ibch.ru or yutkin@yandex.ru; Tel.: +7-495-3355622

**Abstract:** Cardiotoxins (CaTx) of the three-finger toxin family are one of the main components of cobra venoms. Depending on the structure of the N-terminal or the central polypeptide loop, they are classified into either group I and II or P- and S-types, respectively, and toxins of different groups or types interact with lipid membranes variably. While their main target in the organism is the cardiovascular system, there is no data on the effects of CaTx from different groups or types on cardiomyocytes. To evaluate these effects, a fluorescence measurement of intracellular Ca<sup>2+</sup> concentration and an assessment of the rat cardiomyocytes' shape were used. The obtained results showed that CaTx of group I containing two adjacent proline residues in the N-terminal loop were less toxic to cardiomyocytes than group II toxins and that CaTx of S-type were less active than P-type ones. The highest activity was observed for *Naja oxiana* cobra cardiotoxin 2, which is of P-type and belongs to group II. For the first time, the effects of CaTx of different groups and types on the cardiomyocytes were studied, and the data obtained showed that the CaTx toxicity to cardiomyocytes depends on the structures both of the N-terminal and central polypeptide loops.

**Keywords:** cardiotoxin; cardiomyocyte; hypercontracture; calcium concentration



**Citation:** Averin, A.S.; Berezhnov, A.V.; Pimenov, O.Y.; Galimova, M.H.; Starkov, V.G.; Tsetlin, V.I.; Utkin, Y.N. Effects of Cobra Cardiotoxins on Intracellular Calcium and the Contracture of Rat Cardiomyocytes Depend on Their Structural Types. *Int. J. Mol. Sci.* **2023**, *24*, 9259. <https://doi.org/10.3390/ijms24119259>

Academic Editor: Steve Peigneur

Received: 28 April 2023

Revised: 16 May 2023

Accepted: 22 May 2023

Published: 25 May 2023



**Copyright:** © 2023 by the authors. Licensee MDPI, Basel, Switzerland. This article is an open access article distributed under the terms and conditions of the Creative Commons Attribution (CC BY) license (<https://creativecommons.org/licenses/by/4.0/>).

## 1. Introduction

Cobra venom cardiotoxins (cytotoxins, CaTx) are small proteins belonging to the family of three-finger toxins [1]. They are one of the main components of cobra venoms and, in the victim organism, affect the cardiovascular system. The structure of the CaTx molecule is characterized by three  $\beta$ -structured polypeptide loops emerging from a small hydrophobic core stabilized by four disulfide bonds. According to differences in the interaction with zwitterionic phospholipid dispersion, S- and P-types of CaTx were distinguished [2]. The toxins of the S-type comprise a serine residue at position 28 (Figure 1) of the amino acid sequences, and never have proline at position 30, at which usually leucine, lysine, or serine residues are located. CaTx of the P-type contain a proline residue at position 30 and alanine at position 28 in most sequences. On the basis of structural studies, CaTx were classified in two other subclasses, i.e., groups I and II [3,4]. Group I CaTx is characterized by the presence of two proline residues at position 8 and 9 as well as an aromatic residue (tyrosine or tryptophan) at position 11 of the amino acid sequence. All other CaTx were of group II.



overload results in the development of irreversible hypercontracture (HC), which was observed previously under the action of different toxic agents [13,14] and subsequent dye loss; while, normally, the contraction of a cardiomyocyte usually does not exceed 10% of its length, HC is characterized by a sharp, 2–3 times decrease in the length of the cardiomyocyte and the transition of its shape to an almost spherical one (Figure 2b,e) [15,16]. The cell loses its characteristic structure and the level of fluorescence begins to decrease due to the release of the dye from the cell (Figure 2e).

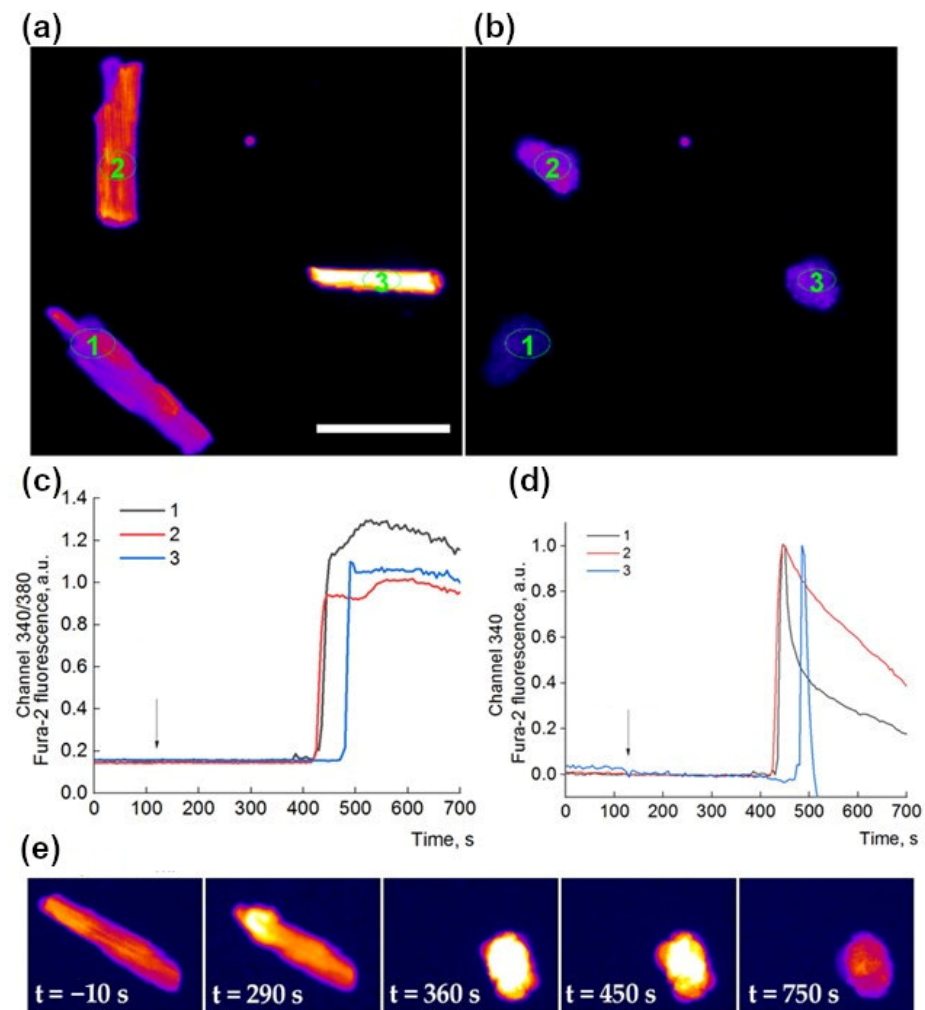


**Figure 2.** Examples of the development of cardiomyocyte  $\text{Ca}^{2+}$  overload, accompanied by HC, under the influence of cardiotoxin. Representative images of three normal cardiomyocytes loaded with Fura-2 (channel 380 only, LUT Fire) (a) and the same hypercontracted cardiomyocytes 380 s after the application of 25  $\mu\text{M}$  CT2No (b). Numbers 1–3 denote individual cardiomyocytes. Ovals depict regions of interest (ROIs). Intracellular ROIs are used for monitoring  $[\text{Ca}^{2+}]_i$  responses and are selected manually. Scale bar—100  $\mu\text{m}$ . The increment in  $[\text{Ca}^{2+}]_i$  registered as 340/380 ratio (c) and in 340 channel (d). Arrows indicate application of 25  $\mu\text{M}$  CT2No. (e) Development of the effect over time after application of 25  $\mu\text{M}$  CT1Nk at  $t = 0$ .

At a concentration of 25  $\mu\text{g}/\text{mL}$ , CT2No and CT1Nk induced HC in 100% of cells while, for CT1No, the proportion of cells with HC was  $89 \pm 13\%$  (Figure 3). CT1Nh and CT2Nh showed a significantly weaker activity, causing HC in  $18 \pm 17\%$  and  $7 \pm 12\%$  of cells, respectively (Figure 3b). It should also be noted that the time of HC onset and the rise in intracellular  $\text{Ca}^{2+}$  concentration was the shortest for CT2No, being  $162 \pm 86$  and  $152 \pm 87$  s. The same parameters for other toxins were:  $312 \pm 148$  and  $299 \pm 137$  s for CT1Nk;  $736 \pm 397$

and  $747 \pm 387$  for CT1No;  $1328 \pm 577$  and  $1255 \pm 615$  for CT2Nh; and  $1522 \pm 177$  and  $1420 \pm 223$  s for CT1Nh. Thus, the toxins studied were divided into 2 groups:

- (1) the group with high activity, which included CT2No, CT1Nk, and CT1No;
- (2) the group with low activity: CT2Nh and CT1Nh.

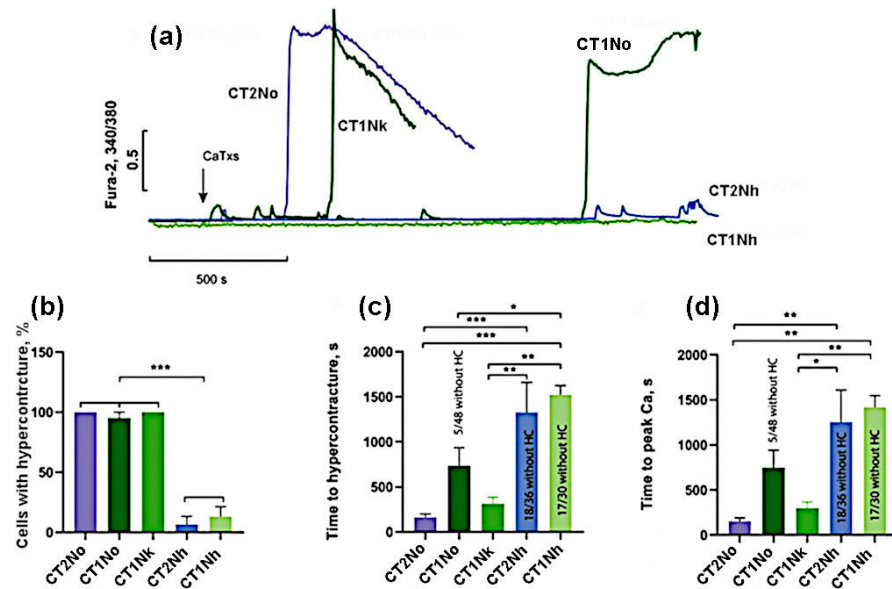


**Figure 3.** Comparison of the effects of CaTxs at a concentration of 25 µg/mL. (a) Typical example of recording a fluorescent Fura-2 signal. Arrow indicates cardiotoxin application. (b) Number of cells with hypercontracture (HC) after 30 min of CaTx application. (c) Time of the onset of the HC. (d) Time to the maximum rate of increase in concentration of intracellular Ca<sup>2+</sup>. CT2No ( $n = 4$ ); CT1Nk ( $n = 4$ ); CT1No ( $n = 4$ ); CT2Nh ( $n = 3$ ); and CT1Nh ( $n = 3$ ). Asterisks indicate the significant differences at \*  $p < 0.05$ , \*\*  $p < 0.01$ , and \*\*\*  $p < 0.005$ .

For a more accurate comparison of the activities for the toxins of the first group, we carried out additional experiments at a lower (10 µg/mL) concentration of toxins. As can be seen from Figure 4, at this concentration, cardiotoxins CT2No and CT1Nk caused HC in 100% of cells while, for CT1No, the number of cells with HC was  $24 \pm 21\%$ . The time of onset of HC and the rise in intracellular Ca<sup>2+</sup> was the shortest for CT2No ( $393 \pm 207$  and  $396 \pm 217$  s); it was slightly longer for CT1Nk— $503 \pm 307$  and  $520 \pm 318$  s, and reached  $933 \pm 707$  and  $909 \pm 634$  s for CT1No. These results suggest that CT2No and CT1Nk toxins are very similar in their ability to induce HC and Ca<sup>2+</sup> overload in cardiomyocytes and are significantly more active than CT1No.

To compare CT2Nh and CT1Nh toxins possessing fewer pronounced cytotoxic properties, their higher concentrations (100 µg/mL) were used. As can be seen in Figure 5, at this concentration, CT2Nh induced HC in 100% of cells while, for CT1Nh, the proportion of cells with HC was  $74 \pm 29\%$ , but this difference is not statistically significant. The time of onset of HC and the time of rise in intracellular Ca<sup>2+</sup> for CT2Nh were  $531 \pm 148$  and  $518 \pm 163$  s, and for CT1Nh these times were  $1132 \pm 342$  and  $1151 \pm 295$  s, respectively, the observed difference between the two toxins being statistically significant. These results suggest that CT2Nh is much stronger than CT1Nh in its cytotoxic activity against cardiomyocytes.

The data obtained (summarized in Table 1) allow us to propose the following series of CaTx cytotoxicity against rat cardiomyocytes: CT2No=CT1Nk>CT1No>CT2Nh>CT1Nh.

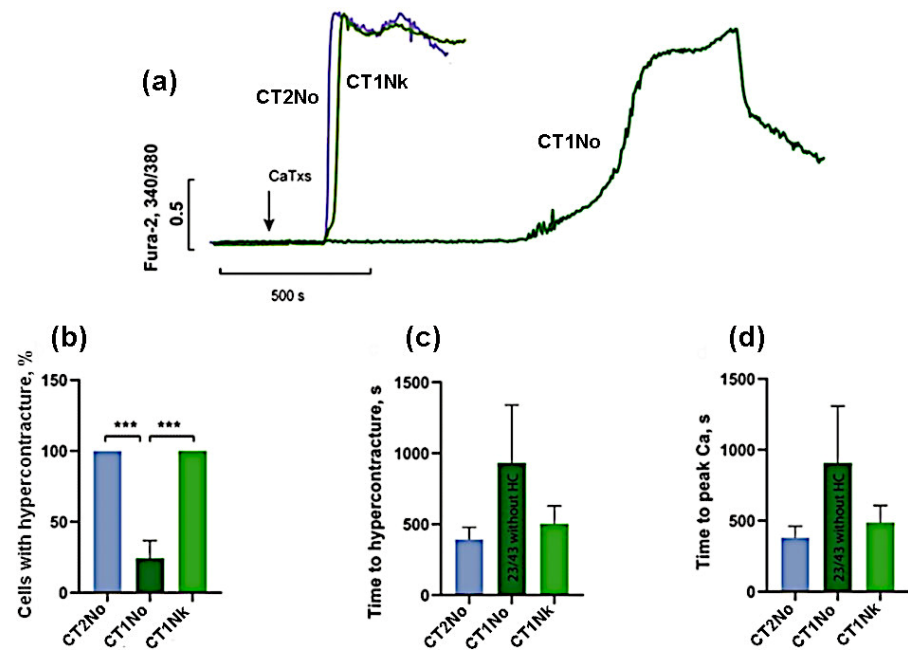


**Figure 4.** Comparison of the CaTx effects at a concentration of 10 µg/mL. (a) Typical example of recording a fluorescent Fura-2 signal. An arrow indicates application of cardiotoxins. (b) Number of cells with HC after 30 min of CaTx application (c) Time of the onset of the HC. (d) Time to the maximum rate of increase in concentration of intracellular Ca<sup>2+</sup>. CT2No (n = 6); CT1Nk (n = 6); and CT1No (n = 3). Asterisks indicate the significant differences at \*\*\* p < 0.005.

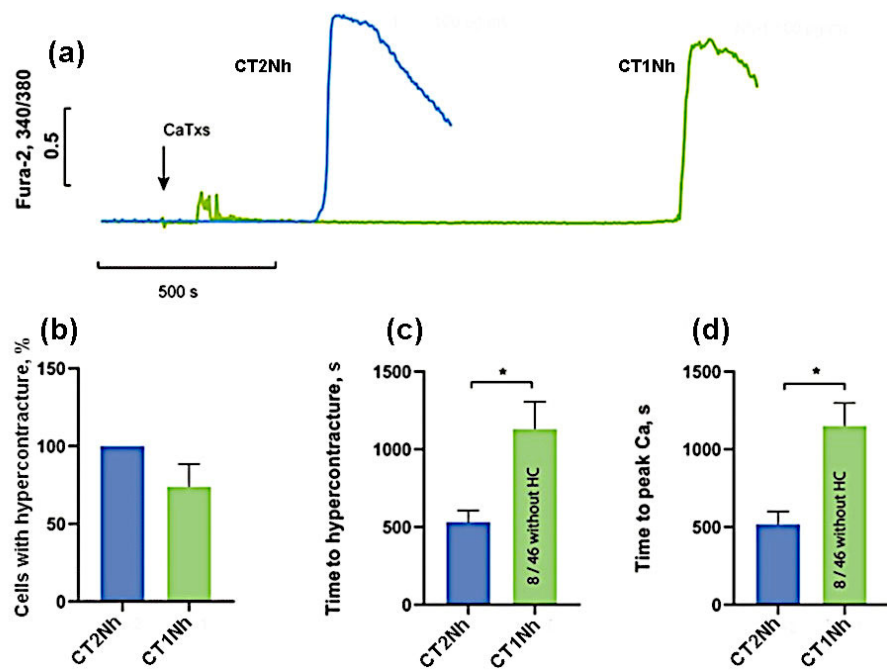


**Figure 5.** Comparison of the effects of CaTxs at a concentration of 100 µg/mL. (a) Typical example of recording a fluorescent Fura-2 signal. An arrow indicates the application of cardiotoxins. (b) Number of cells with HC after 30 min of CaTx application. (c) Time of the onset of the HC. (d) Time to the maximum rate of increase in the concentration of intracellular Ca<sup>2+</sup>. CT2Nh (n = 4) and CT1Nh (n = 4). Asterisks indicate the significant differences at \* p < 0.05.

**Table 1.** Effects of CaTxs at different concentrations on cardiomyocytes.

Toxin	Concentration	Parameter		
		Cells with Hypercontracture, %	Time to Hypercontracture, s	Time to Peak of Ca <sup>2+</sup> Concentration, s
CT2No	10 µg/mL	100	393 ± 207	396 ± 217
	25 µg/mL	100	162 ± 86	152 ± 87
CT1Nk	10 µg/mL	100	503 ± 307	520 ± 318
	25 µg/mL	100	312 ± 148	299 ± 137
CT1No	10 µg/mL	24 ± 21	933 ± 707	909 ± 634
	25 µg/mL	89 ± 13	736 ± 397	747 ± 387
CT2Nh	25 µg/mL	18 ± 17	1328 ± 577	1255 ± 615
	100 µg/mL	100	531 ± 148	518 ± 163
CT1Nh	25 µg/mL	7 ± 12	1522 ± 177	1420 ± 223
	100 µg/mL	74 ± 29	1132 ± 342	1151 ± 295

### 3. Discussion

The homeostasis of Ca<sup>2+</sup> ions plays an important role in the functioning of the heart in general and cardiomyocytes in particular. The disturbance of calcium homeostasis in cardiomyocytes can lead to the appearance of uncontrolled heart contractions and, thus, a disruption of the normal function of the heart muscle. The available evidence indicates that cobra CaTxs disrupt the calcium homeostasis of cardiomyocytes. The action of toxins results in a calcium overload followed by HC and cell death [10]. The action of cardiotoxins on the heart muscles leads to a disruption of their contractions and contracture and, by acting on the heart, these toxins cause a systolic heart arrest. Earlier, we studied the effects of CT1No and CT2No on the rat papillary muscle and showed that both toxins produced contracture at a concentration of 5 µg/mL [8]. These CaTxs are of different types, CT1No of S-type and CT2No of P-type, and, against papillary muscle, CT2No was more active. On the isolated rat heart, perfused according to the Langendorff technique, CT2No was also more active than CT1No [7]. In the present work, we extended our studies to cardiomyocytes and supplemented the set of toxins by three more CaTxs.

As mentioned in the introduction, the CaTxs are the main components in the majority of cobra venoms. For example, in the venom of the Nigerian *N. nigricollis* cobra, CaTxs comprise more than 70% of proteins [17]. As concerns the toxins used in our study, the content of CT1No and CT2No in the crude *N. oxiana* venom is 15 and 18%, respectively [18]. According to the proteomic data, CT1Nk accounts for more than 20% of all proteins in the *N. kaouthia* venom [19]. The proteomic analysis of *N. haje* venom showed that the three-finger toxins to which CaTxs belong constitute 52% of the total venom proteins [20], and CaTxs make up more than 50% of the three-finger toxins [21]. That is, the content of CT1Nh and CT2Nh in the *N. haje* venom is a few dozen percent.

The toxin concentrations applied here for cardiomyocytes were higher than those (5 µg/mL) affecting the function of the papillary muscle and heart. This difference can be explained by the fact that cardiomyocytes were at rest, while the papillary muscle contracted rhythmically under the influence of electrical stimuli. Since, in work on mouse cardiomyocytes, an increase in the frequency of stimulation increased the diastolic calcium level and calcium content in the sarcoplasmic reticulum (SR) [16], it could be expected that, under conditions of electrical stimulation to trigger contracture, a lower influx of calcium induced by cardiotoxins would be required. All the toxins studied in this work produced an increase in intracellular calcium and the development of contracture, these effects being similar to those observed earlier [10]. The release of calcium from the SR and the entry of extracellular calcium through various mechanisms contribute to the creation of calcium overload [8,10]. Earlier, on the isolated rat heart, perfused according to the Langendorff technique [9], we observed that CT1No and CT2No produced a transient increase in pulse pressure and an increase in diastolic pressure without changing the heart rate. Finally, both

toxins caused heart contracture. It may be expected that the effects of other CaTxs studied in the present work on the whole heart will be similar.

The diversified actions of cardiotoxins should also be noted. In addition to calcium overload, they can interact with mitochondria, disrupting their function [22,23], which may also cause cardiotoxic effects [14]. However, as we have shown earlier [8], it is the blocking of the entry of extracellular calcium that prevents irreversible damage to the myocardium. That is, it is this process that plays a leading role in the development of pathological disorders. A further chain of pathological disorders may include the increase in reactive oxygen species [23], as well as the activation of peptidases [24,25], leading to irreversible contracture and cell death [10,26]. Cardiomyocyte HC is an excessive cell shortening. The development of cardiomyocyte HC is an essential mechanism of the reperfusion-induced injury. HC can propagate to adjacent cells through gap junctions [27] and is an important mechanism of myocyte death during reperfusion. Reperfusion-induced HC may originate from  $\text{Ca}^{2+}$  overload, when energy recovery is rapid but cytosolic  $\text{Ca}^{2+}$  load is high [28,29]. A similar phenomenon is seen in the action of CaTxs on cardiomyocytes. It should be mentioned that reperfused myocardial infarcts consist almost exclusively of areas of contraction band necrosis formed by hypercontracted dead cardiomyocytes [30]. Cobra CaTxs causes cardiomyocyte HC and death, and this situation is similar to that which one might see in reperfusion heart injury.

The available data suggest that the *in vivo* toxicity of CaTxs can vary quite a lot (e.g., [31]), but it may depend on many parameters, not only on the CaTx effects on the heart. It is even more difficult to interpret the changes that occur in the cardiovascular system when exposed to the whole venom since, in addition to cardiotoxins, cobra venom contains neurotoxins, PLA2, and many other components [32,33] which can affect the heart. In experiments on mice, the venom of the cobra *N. sputatrix* had a pronounced cardiotoxic effect, causing bradycardia, an increase in the amplitude of QRS complexes, and cardiac arrhythmias [34]. However, it is difficult to accurately determine this effect exclusively with cardiotoxins since cardiotoxic effects have been shown for many PLA2s [35,36].

In clinical practice, cobra bites tend to be dominated by neurotoxic effects, and the main efforts are directed towards maintaining respiration, with much less attention paid to cardiovascular effects [37,38]. Nevertheless, there are cases with pronounced cardiotoxic effects [39,40]. At the same time, as a result of therapy directed primarily against neurotoxic components, the significance of cardiotoxic effects increases [41]. This leads to the idea that the identification of the most active cardiotoxins can be useful in understanding the species specificity of the development of the pathological effects of cobra envenomation and can provide an additional criterion for evaluating the effectiveness of antivenoms.

The comparative data on the direct effects of various cardiotoxins on cardiac muscle or on the heart are very limited. As already noted, we showed that a P-type cardiotoxin had greater cardiotoxicity than that of the S-type [7,8]. This difference is explained by the greater membrane-damaging effect of the P-type CaTxs as compared to the S-type ones [5], i.e., the structure of the central polypeptide loop II (Figure 1) determines the CaTx activity. Recently, we demonstrated that the N-terminal loop I also plays an important role in the membrane-damaging activity of CaTxs [6]. We found that CaTxs of group I with a Pro-Pro peptide bond in loop I exhibited attenuated membrane-perturbing activity in model membranes, and lower cytotoxic/antibacterial activity than the CaTx of group II with a single Pro-residue in the loop I [6]. In the present work, we show that differences in the structure of both loop I and loop II determine the cardiotoxic effects of CaTxs. Therefore, CT2No demonstrated the highest toxicity to cardiomyocytes, this toxin being of the P-type from group II. The least active was CT1Nh of the S-type from group I. Three other CaTxs occupied intermediate places depending on the type and group (Table 1).

Interestingly, S-type CT1Nk was more potent than the S-type CT1No. The main differences between these two toxins are in the structure of loop I. Thus, Ser-11 in CT1Nk is changed to Tyr-11 in CT1No (Figure 1). Such a bulky aromatic residue may complicate the insertion of the loop into the membrane, reducing the general cytotoxic effect. The

difference in the activity between CT1Nk and CT1No underlines once more the importance of the loop I structure for the activity of CaTxS.

Although we found a variation in the effects of CaTxS belonging to different types and groups, still only a limited number of toxins of each type and group was used in this work. To find out whether the differences we discovered extend to other toxins, we plan to carry out a study on a larger number of CaTxS.

## 4. Materials and Methods

### 4.1. Materials

Fura-2 was from Invitrogen (cat. no. F1221, Eugene, OR, USA). Coverslips Menzel-Gläser Ø25 mm #1 were from Thermo Scientific (Darmstadt, Germany). All salts and other reagents were purchased from PanEco (Moscow, Russia).

Cardiotoxins were isolated from cobra venoms as described [6]. The structures of isolated CaTxS were confirmed by mass spectrometry and purity by analytical reversed phase HPLC.

### 4.2. Cardiomyocyte Preparation

Hearts were dissected from anesthetized animals (pentobarbital, 50 mg/kg i.p.), and solutions for retrograde perfusion and ventricular myocytes isolation were prepared based on a “low-Ca<sup>2+</sup> medium” containing (in mM): NaCl, 80; KCl, 10; KH<sub>2</sub>PO<sub>4</sub>, 1.2; MgSO<sub>4</sub>, 5; glucose, 20; taurine, 50; L-arginine, 1; and HEPES, 10 (pH 7.2), as described previously [42]. Isolated cardiomyocytes were stored in low-Ca<sup>2+</sup> medium supplemented with 200 µM CaCl<sub>2</sub>. Only rod-shaped cardiomyocytes with clear striations were used. Cells were stored at 4 °C in low calcium Hanks’ balanced salt solution (HBSS) with the following composition (in mM): 138 NaCl, 1.3 CaCl<sub>2</sub>, 0.4 MgSO<sub>4</sub>, 0.5 MgCl<sub>2</sub>, 5.3 KCl, 0.45 KH<sub>2</sub>PO<sub>4</sub>, 4 NaHCO<sub>3</sub>, 0.3 Na<sub>2</sub>HPO<sub>4</sub>, 10 glucose, and 20 HEPES (pH 7.36 at 29–30 °C was adjusted with NaOH). The cells were used for study within 6–7 h after isolation.

### 4.3. Dye Loading

For staining with a fluorescent calcium-sensitive ratiometric probe Fura-2, the cells were placed in the center of a round cover slip with a diameter of 25 mm and a thickness of 0.17 mm in a drop of 200 µL, then the cells were allowed to precipitate for 2 min. Using a pipette, the medium was replaced with 200 µL of HBSS containing 5 µM Fura-2AM. Cells were incubated for 40 min at 30 °C in the dark. Then, the medium was replaced with HBSS without dye with a pipette, a coverslip was mounted in a special measuring cell for an inverted microscope, and the cells were washed again. The volume of the medium was adjusted to 1 mL and the measuring cell was placed on the microscope stage for the experiment.

### 4.4. Fluorescence Microscopy

Fura-2 fluorescence in cardiomyocytes was measured using a Cell Observer fluorescent station based on an AxioVert 200 M motorized inverted microscope (Carl Zeiss AG, Oberkochen, Germany) equipped with a 10× PlanApochromat objective, an Orca-Flash R2 monochrome camera (Hamamatsu Photonics K.K., Iwata City, Japan), and a system for a high-speed change in excitatory filters Ludl MAC 5000 (Ludl Electronic Products, Hawthorne, NY, USA). Fura-2 fluorescence was excited with an HBO100 mercury lamp in two channels using a set of 21HE light filters (Carl Zeiss AG, Oberkochen, Germany): excitation 1—340 ± 15 nm (channel 340); excitation 2—387 ± 8 nm (channel 380); FT 409 beam splitter; and 510 ± 45 nm emission filter. The exposure time for each of the channels was 100 ms. The registration frequency was 1 frame per 5 s. The power of the light source was set to the minimum value that provided an acceptable signal-to-noise ratio. In control experiments with the selected recording parameters, no effect of illumination on the Fura-2 signal was detected for 30 min or more.

#### 4.5. Reagents Application

To ensure uniform distribution of the added CaTx in the cell incubation medium, the substances were applied as follows: from 1 mL of HBSS in the measuring cell, half was taken, and a solution of CaTx with double concentration was prepared in a separate microtube. After that, the CaTx solution was returned to the measuring cell and gently mixed twice with a micropipette. In the control experiments, no noticeable effect of the taking and mixing of the medium on the Fura-2 signal was observed.

#### 4.6. Image Processing

The two-channel series of images was processed in Image J/Fiji (NIH, Bethesda, MD, USA). After determining and subtracting the background signal, the images were smoothed with a simple anti-aliasing filter with a  $3 \times 3$  px grid and the ratio of the data for the 340 nm channel to those of the 380 nm channel, in 32-bit format, was calculated. Next, ROIs (regions of interest) corresponding to the position of the cardiomyocyte were selected in order to capture only the area of the cell, regardless of its movement during the contraction. A table of the ratio of Fura-2 fluorescence signals at 340 and 380 nm excitation versus time was calculated. In some cases, to determine the moment of destruction of the integrity of the plasmalemma by the outflow of the fluorescent probe, the channel for registering the calcium-bound form of the dye (channel 340) was used. Origin 2016 (OriginLab Corporation, Northampton, MA, USA) and GraphPad Prism 8 (GraphPad Software Inc., Boston, MA, USA) were used to plot the graphs.

#### 4.7. Data Analysis and Statistics

Paired *t*-test and one-way ANOVA with Tukey's post hoc test were used for the comparison of two or multiple groups, respectively. The difference was considered statistically significant at  $p < 0.05$ . All data are presented as mean  $\pm$  standard error (S.E.)

### 5. Conclusions

Thus, a comparison of the effects of CaTxs of different types and groups on rat cardiomyocytes showed that the P-type toxins produced stronger effects than the S-type ones, and that group II toxins were more active than those of group I. All toxins exerted close impacts on the cardiomyocyte calcium overload and contracture. However, the effects strongly depended on the structures of the loops I and II. We suggest that CaTxs of the P-type (with Pro30 in the loop II) from group II (with one Pro9 in loop I) possess the highest toxicity. The observed variations may be explained by the differences in the membrane-damaging activity of CaTxs.

**Author Contributions:** Conceptualization, A.S.A. and A.V.B.; methodology, A.S.A.; investigation, A.S.A., A.V.B., O.Y.P. and M.H.G.; resources, V.G.S.; writing—original draft preparation, A.S.A.; writing—review and editing, V.I.T. and Y.N.U.; supervision, V.I.T.; project administration, Y.N.U.; funding acquisition, Y.N.U. All authors have read and agreed to the published version of the manuscript.

**Funding:** This research was funded by Russian Science Foundation (RSF), grant number 21-14-00316.

**Institutional Review Board Statement:** The study was conducted in accordance with the Declaration of Helsinki, and approved by the Biological Safety and Ethics Committee of the Institute of Cell Biophysics (Instruction for the use of laboratory animals in the Institute of Cell Biophysics No 57 of 30 December 2011).

**Informed Consent Statement:** Not applicable.

**Data Availability Statement:** All data obtained in this study are contained within the article.

**Conflicts of Interest:** The authors declare no conflict of interest. The funders had no role in the design of the study; in the collection, analyses, or interpretation of data; in the writing of the manuscript; or in the decision to publish the results.

## References

1. Kalita, B.; Utkin, Y.N.; Mukherjee, A.K. Current Insights in the Mechanisms of Cobra Venom Cytotoxins and Their Complexes in Inducing Toxicity: Implications in Antivenom Therapy. *Toxins* **2022**, *14*, 839. [[CrossRef](#)] [[PubMed](#)]
2. Chien, K.Y.; Chiang, C.M.; Hseu, Y.C.; Vyas, A.A.; Rule, G.S.; Wu, W. Two distinct types of cardiotoxin as revealed by the structure and activity relationship of their interaction with zwitterionic phospholipid dispersions. *J. Biol. Chem.* **1994**, *269*, 14473–14483. [[CrossRef](#)] [[PubMed](#)]
3. Chen, T.-S.; Chung, F.-Y.; Tjong, S.-C.; Goh, K.-S.; Huang, W.-N.; Chien, K.-Y.; Wu, P.-L.; Lin, H.-C.; Chen, C.-J.; Wu, W. Structural difference between group I and group II cobra cardiotoxins: X-ray, NMR, and CD analysis of the effect of cis-proline conformation on three-fingered toxins. *Biochemistry* **2005**, *44*, 7414–7426. [[CrossRef](#)] [[PubMed](#)]
4. Grognet, J.M.; Ménez, A.; Drake, A.; Hayashi, K.; Morrison, I.E.; Hider, R.C. Circular dichroic spectra of elapid cardiotoxins. *Eur. J. Biochem.* **1988**, *172*, 383–388. [[CrossRef](#)]
5. Dubovskii, P.V.; Lesovoy, D.M.; Dubinnyi, M.A.; Konshina, A.G.; Utkin, Y.N.; Efremov, R.G.; Arseniev, A.S. Interaction of three-finger toxins with phospholipid membranes: Comparison of S- and P-type cytotoxins. *Biochem. J.* **2005**, *387*, 807–815. [[CrossRef](#)]
6. Dubovskii, P.V.; Ignatova, A.A.; Alekseeva, A.S.; Starkov, V.G.; Boldyrev, I.A.; Feofanov, A.V.; Utkin, Y.N. Membrane-Disrupting Activity of Cobra Cytotoxins Is Determined by Configuration of the N-Terminal Loop. *Toxins* **2022**, *15*, 6. [[CrossRef](#)]
7. Averin, A.S.; Astashev, M.E.; Andreeva, T.V.; Tsetlin, V.I.; Utkin, Y.N. Cardiotoxins from Cobra *Naja oxiana* Change the Force of Contraction and the Character of Rhythmoinotropic Phenomena in the Rat Myocardium. *Dokl. Biochem. Biophys.* **2019**, *487*, 282–286. [[CrossRef](#)]
8. Averin, A.S.; Nenov, M.N.; Starkov, V.G.; Tsetlin, V.I.; Utkin, Y.N. Effects of Cardiotoxins from *Naja oxiana* Cobra Venom on Rat Heart Muscle and Aorta: A Comparative Study of Toxin-Induced Contraction Mechanisms. *Toxins* **2022**, *14*, 88. [[CrossRef](#)]
9. Averin, A.S.; Goltyaev, M.V.; Andreeva, T.V.; Starkov, V.G.; Tsetlin, V.I.; Utkin, Y.N. S- and P-type cobra venom cardiotoxins differ in their action on isolated rat heart. *J. Venom. Anim. Toxins Incl. Trop. Dis.* **2022**, *28*, e20210110. [[CrossRef](#)]
10. Tzeng, W.F.; Chen, Y.H. Suppression of snake-venom cardiotoxin-induced cardiomyocyte degeneration by blockage of Ca<sup>2+</sup> influx or inhibition of non-lysosomal proteinases. *Biochem. J.* **1988**, *256*, 89–95. [[CrossRef](#)]
11. Wang, H.X.; Lau, S.Y.; Huang, S.J.; Kwan, C.Y.; Wong, T.M. Cobra venom cardiotoxin induces perturbations of cytosolic calcium homeostasis and hypercontracture in adult rat ventricular myocytes. *J. Mol. Cell. Cardiol.* **1997**, *29*, 2759–2770. [[CrossRef](#)] [[PubMed](#)]
12. Wang, C.-H.; Wu, W.-g. Amphiphilic beta-sheet cobra cardiotoxin targets mitochondria and disrupts its network. *FEBS Lett.* **2005**, *579*, 3169–3174. [[CrossRef](#)] [[PubMed](#)]
13. Berezhnov, A.V.; Fedotova, E.I.; Nenov, M.N.; Kasymov, V.A.; Pimenov, O.Y.; Dynnik, V.V. Dissecting Cellular Mechanisms of Long-Chain Acylcarnitines-Driven Cardiotoxicity: Disturbance of Calcium Homeostasis, Activation of Ca<sup>2+</sup>-Dependent Phospholipases, and Mitochondrial Energetics Collapse. *Int. J. Mol. Sci.* **2020**, *21*, 7461. [[CrossRef](#)] [[PubMed](#)]
14. Ruiz-Meana, M.; Abellán, A.; Miró-Casas, E.; Garcia-Dorado, D. Opening of mitochondrial permeability transition pore induces hypercontracture in Ca<sup>2+</sup> overloaded cardiac myocytes. *Basic Res. Cardiol.* **2007**, *102*, 542–552. [[CrossRef](#)] [[PubMed](#)]
15. Antoons, G.; Mubagwa, K.; Nevelsteen, I.; Sipido, K.R. Mechanisms underlying the frequency dependence of contraction and Ca(2+)(i) transients in mouse ventricular myocytes. *J. Physiol.* **2002**, *543*, 889–898. [[CrossRef](#)] [[PubMed](#)]
16. Picht, E.; DeSantiago, J.; Huke, S.; Kaetzel, M.A.; Dedman, J.R.; Bers, D.M. CaMKII inhibition targeted to the sarcoplasmic reticulum inhibits frequency-dependent acceleration of relaxation and Ca<sup>2+</sup> current facilitation. *J. Mol. Cell. Cardiol.* **2007**, *42*, 196–205. [[CrossRef](#)]
17. Petras, D.; Sanz, L.; Segura, A.; Herrera, M.; Villalta, M.; Solano, D.; Vargas, M.; León, G.; Warrell, D.A.; Theakston, R.D.G.; et al. Snake venomomics of African spitting cobras: Toxin composition and assessment of congeneric cross-reactivity of the pan-African EchiTAB-Plus-ICP antivenom by antivenomics and neutralization approaches. *J. Proteome Res.* **2011**, *10*, 1266–1280. [[CrossRef](#)]
18. Grishin, E.V.; Sukhikh, A.P.; Adamovich, T.B.; Ovchinnikov, Y.A. Isolation, properties, and amino acid sequence of two cytotoxins from the venom of the Central Asian cobra *Naja oxiana*. *Bioorg. Khim.* **1976**, *2*, 1018–1034.
19. Ryabinin, V.V.; Ziganshin, R.H.; Starkov, V.G.; Tsetlin, V.I.; Utkin, Y.N. Intraspecific Variability in the Composition of the Venom from Monocled Cobra (*Naja kaouthia*). *Russ. J. Bioorg. Chem.* **2019**, *45*, 107–121. [[CrossRef](#)]
20. Adamude, F.A.; Dingwoke, E.J.; Abubakar, M.S.; Ibrahim, S.; Mohamed, G.; Klein, A.; Sallau, A.B. Proteomic analysis of three medically important Nigerian *Naja* (*Naja haje*, *Naja katiensis* and *Naja nigricollis*) snake venoms. *Toxicon* **2021**, *197*, 24–32. [[CrossRef](#)]
21. Malih, I.; Rusmili, A.M.R.; Tee, T.Y.; Saile, R.; Ghalim, N.; Othman, I. Proteomic analysis of Moroccan cobra *Naja haje legionis* venom using tandem mass spectrometry. *J. Proteom.* **2014**, *96*, 240–252. [[CrossRef](#)] [[PubMed](#)]
22. Gasanov, S.E.; Shrivastava, I.H.; Israilov, F.S.; Kim, A.A.; Rylova, K.A.; Zhang, B.; Dagda, R.K. *Naja naja oxiana* Cobra Venom Cytotoxins CTI and CTII Disrupt Mitochondrial Membrane Integrity: Implications for Basic Three-Fingered Cytotoxins. *PLoS ONE* **2015**, *10*, e0129248. [[CrossRef](#)]
23. Fakhri, A.; Omranipour, R.; Fakhri, S.; Mirshamsi, M.; Zangeneh, F.; Vatanpour, H.; Pourahmad, J. *Naja Naja Oxiana* Venom Fraction Selectively Induces ROS-Mediated Apoptosis in Human Colorectal Tumor Cells by Directly Targeting Mitochondria. *Asian Pac. J. Cancer Prev.* **2017**, *18*, 2201–2208. [[CrossRef](#)] [[PubMed](#)]
24. Shi, Y.-J.; Huang, C.-H.; Lee, Y.-C.; Wang, L.-J.; Chiou, J.-T.; Chang, L.-S. *Naja atra* cardiotoxins enhance the protease activity of chymotrypsin. *Int. J. Biol. Macromol.* **2019**, *136*, 512–520. [[CrossRef](#)] [[PubMed](#)]
25. Harvey, A.L.; Marshall, R.J.; Karlsson, E. Effects of purified cardiotoxins from the Thailand cobra (*Naja naja siamensis*) on isolated skeletal and cardiac muscle preparations. *Toxicon* **1982**, *20*, 379–396. [[CrossRef](#)] [[PubMed](#)]

26. Wang, C.-H.; Monette, R.; Lee, S.-C.; Morley, P.; Wu, W.-g. Cobra cardiotoxin-induced cell death in fetal rat cardiomyocytes and cortical neurons: Different pathway but similar cell surface target. *Toxicon* **2005**, *46*, 430–440. [[CrossRef](#)]
27. Ruiz-Meana, M.; Garcia-Dorado, D.; Hofstaetter, B.; Piper, H.M.; Soler-Soler, J. Propagation of cardiomyocyte hypercontracture by passage of Na(+) through gap junctions. *Circ. Res.* **1999**, *85*, 280–287. [[CrossRef](#)]
28. Kojima, A.; Kitagawa, H.; Omatsu-Kanbe, M.; Matsuura, H.; Nosaka, S. Sevoflurane protects ventricular myocytes against oxidative stress-induced cellular Ca<sup>2+</sup> overload and hypercontracture. *Anesthesiology* **2013**, *119*, 606–620. [[CrossRef](#)]
29. Garcia-Dorado, D.; Ruiz-Meana, M.; Inserte, J.; Rodriguez-Sinovas, A.; Piper, H.M. Calcium-mediated cell death during myocardial reperfusion. *Cardiovasc. Res.* **2012**, *94*, 168–180. [[CrossRef](#)]
30. Solares, J.; Garcia-Dorado, D.; Oliveras, J.; González, M.A.; Ruiz-Meana, M.; Barrabés, J.A.; Gonzalez-Bravo, C.; Soler-Soler, J. Contraction band necrosis at the lateral borders of the area at risk in reperfused infarcts. Observations in a pig model of in situ coronary occlusion. *Virchows Arch.* **1995**, *426*, 393–399. [[CrossRef](#)] [[PubMed](#)]
31. Jayaraman, G.; Kumar, T.K.; Tsai, C.C.; Srisailam, S.; Chou, S.H.; Ho, C.L.; Yu, C. Elucidation of the solution structure of cardiotoxin analogue V from the Taiwan cobra (*Naja naja atra*)-identification of structural features important for the lethal action of snake venom cardiotoxins. *Protein Sci.* **2000**, *9*, 637–646. [[CrossRef](#)] [[PubMed](#)]
32. Tan, C.H.; Wong, K.Y.; Huang, L.-K.; Tan, K.Y.; Tan, N.H.; Wu, W.-g. Snake Venomics and Antivenomics of Cape Cobra (*Naja nivea*) from South Africa: Insights into Venom Toxicity and Cross-Neutralization Activity. *Toxins* **2022**, *14*, 860. [[CrossRef](#)] [[PubMed](#)]
33. Deka, A.; Gogoi, A.; Das, D.; Purkayastha, J.; Doley, R. Proteomics of *Naja kaouthia* venom from North East India and assessment of Indian polyvalent antivenom by third generation antivenomics. *J. Proteom.* **2019**, *207*, 103463. [[CrossRef](#)] [[PubMed](#)]
34. Cher, C.D.N.; Armugam, A.; Zhu, Y.Z.; Jeyaseelan, K. Molecular basis of cardiotoxicity upon cobra envenomation. *Cell. Mol. Life Sci.* **2005**, *62*, 105–118. [[CrossRef](#)]
35. Fletcher, J.E.; Yang, C.C.; Rosenberg, P. Basic phospholipase A2 from *Naja nigricollis* snake venom: Phospholipid hydrolysis and effects on electrical and contractile activity of the rat heart. *Toxicol. Appl. Pharmacol.* **1982**, *66*, 39–54. [[CrossRef](#)]
36. Karabuva, S.; Lukšić, B.; Brizić, I.; Latinović, Z.; Leonardi, A.; Križaj, I. Ammodytin L is the main cardiotoxic component of the *Vipera ammodytes ammodytes* venom. *Toxicon* **2017**, *139*, 94–100. [[CrossRef](#)]
37. Greene, S.C.; Osborn, L.; Bower, R.; Harding, S.A.; Takenaka, K. Monocled Cobra (*Naja kaouthia*) Envenomations Requiring Mechanical Ventilation. *J. Emerg. Med.* **2021**, *60*, 197–201. [[CrossRef](#)]
38. Kumar, T.K.; Jayaraman, G.; Lee, C.S.; Arunkumar, A.I.; Sivaraman, T.; Samuel, D.; Yu, C. Snake venom cardiotoxins-structure, dynamics, function and folding. *J. Biomol. Struct. Dyn.* **1997**, *15*, 431–463. [[CrossRef](#)]
39. Ismail, A.K.; Weinstein, S.A.; Auliya, M.; Appareo, P. Ventricular bigeminy following a cobra envenomation. *Clin. Toxicol.* **2012**, *50*, 518–521. [[CrossRef](#)]
40. John Binu, A.; Kumar Mishra, A.; Gunasekaran, K.; Iyadurai, R. Cardiovascular manifestations and patient outcomes following snake envenomation: A pilot study. *Trop. Doct.* **2019**, *49*, 10–13. [[CrossRef](#)]
41. Le, H.Q.; Nguyen, N.T.T.; Vo, T.N.A.; van Nguyen, T.; Do, K.T.N.; Ho, T.T.C.; Nguyen, S.N.; Phan, X.T.; Nguyen, D.L.M.; Kieu, D.N.; et al. Envenoming by king cobras (*Ophiophagus hannah*) in Vietnam with cardiac complications and necrotizing fasciitis. *Toxicon* **2021**, *200*, 127–133. [[CrossRef](#)] [[PubMed](#)]
42. Alekseev, A.E.; Korystova, A.F.; Mavlyutova, D.A.; Kokoz, Y.M. Potential-dependent Ca<sup>2+</sup> currents in isolated heart cells of hibernators. *Biochem. Mol. Biol. Int.* **1994**, *33*, 365–375. [[PubMed](#)]

**Disclaimer/Publisher’s Note:** The statements, opinions and data contained in all publications are solely those of the individual author(s) and contributor(s) and not of MDPI and/or the editor(s). MDPI and/or the editor(s) disclaim responsibility for any injury to people or property resulting from any ideas, methods, instructions or products referred to in the content.